Nanoscale

www.rsc.org/nanoscale

Volume 3 | Number 7 | July 2011 | Pages 2645–2984

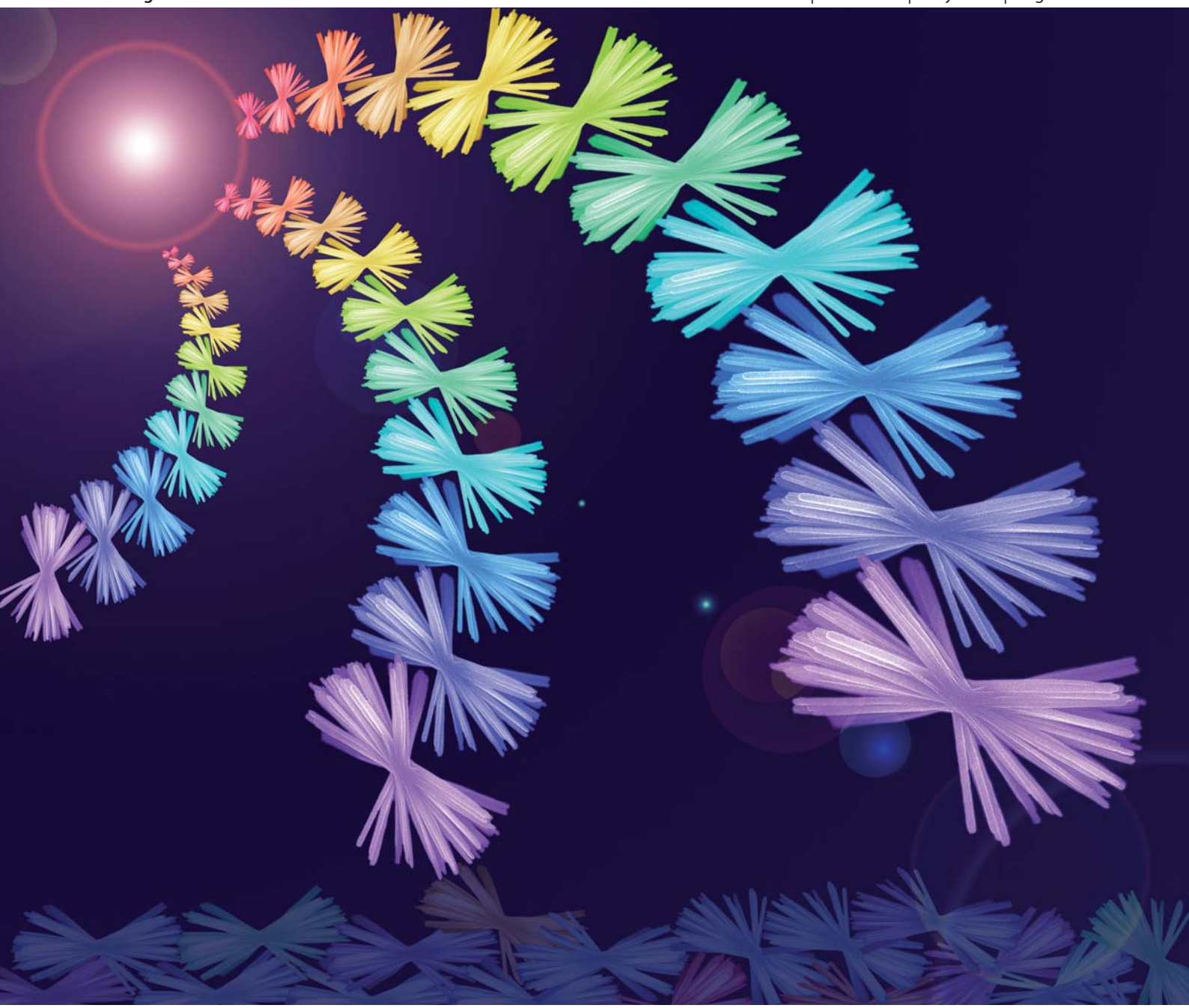

ISSN 2040-3364

COVER ARTICLE

Sun *et al.*

Hierarchical self-assembly of CdTe quantum dots into hyperbranched nanobundles

RSC Publishing

NCNST

Nanoscale

Dynamic Article Links

Cite this: *Nanoscale*, 2011, **3**, 2882

www.rsc.org/nanoscale

PAPER

Hierarchical self-assembly of CdTe quantum dots into hyperbranched nanobundles: Suppression of biexciton Auger recombination†

Ling-Yun Pan,[ab] Yong-Lai Zhang,[a] Hai-Yu Wang,*[a] Hong Liu,[b] Jing-Shan Luo,[b] Hong Xia,[a] Lei Zhao,[c] Qi-Dai Chen,[a] Shu-Ping Xu,[d] Bing-Rong Gao,[a] Li-Min Fu[e] and Hong-Bo Sun*[ab]

Received 31st January 2011, Accepted 31st March 2011
DOI: 10.1039/c1nr10121h

In this paper, we report a novel nanobundle structure formed by the hierarchical self-assembly of TGA-capped CdTe quantum dots. HR-TEM confirms the polycrystalline phase of the bundle structure, and that pristine quantum dots are the building units. The steady state absorption and luminescence properties of the pristine quantum dots can be well inherited by the nanobundles. In transient state observation, carrier quenching induced by Auger recombination is found to be remarkably suppressed. Electron delocalizing to close building units is considered to be the reason. Suppression of Auger recombination may earn much more time for charge separation, which makes the novel nanobundle structures suitable for the excellent donor material in solar cell applications.

1. Introduction

As a result of their optical tunability,[1,2] exciton multiplication efficiency[3,4] and heterostructure compatability,[5] semiconductor quantum dots (QDs) are promising materials for the next generation solar cells.[6,7] However, when QDs are combined with conjugated polymers in donor–acceptor heterojunctions, monodisperse semiconductor QDs suffer from short carrier diffusion lengths, because of phase separation during device preparation. This generally leads to carrier recombination before the electron transport, and thus a significant decrease in the efficiency of the photovoltaic conversion.[5,8,9] Therefore, very high loading contents of semiconductor QDs, as well as long carrier diffusion lengths, are generally required to provide interconnected structures. As inspired from natural plants, for example large surface or high aspect-ratio leaves are effective for photosynthesis, hyperbranched semiconductor nanostructures were successfully fabricated to improve the light harvesting efficiency and the charge separation efficiency.[10,11] In these branched networks, carriers could be extracted at much lower loading concentrations, due to their intrinsic percolated structures, allowing the carriers to reach the electrodes without recombination. Thus each hyperbranched structure acts as a small, yet fully functional, hybrid solar cell, and all of them connect in parallel to build up a full photovoltaic conversion circuit.[10,11]

The fabrication of such kinds of three-dimensional (3D) hierarchical nanostructures has progressed greatly thanks to the development of the bottom-up approach.[12–16] Recently, a novel crystallization route, named "nonclassical crystallization" by Cöelfen and Mann,[17,18] has been reported for nanostructuring. In this process, QDs are used as building blocks for the construction of whole hierarchical structures, instead of the ions or single molecules used in conventional crystallization.[19] Nonclassical crystallization involves processes of QD aggregation, self-assembly and mesoscale transformation, and thus the electrical and optical properties of the hierarchical structures can be achieved in a controlled fashion.[19] Based on this unique nonclassical crystallization method, a wide range of semiconductor QDs have been assembled into various hierarchical nanostructures.[20] For example, one-dimensional (1D) CdTe nanostructures such as nanofibres,[21] nanorods[22] and nanotubes[23] have been successfully created with the assistance of ligands[22] or templates.[23] Driven by dipole–dipole interactions and directional hydrophobic attractions, a two-dimensional (2D) CdTe free-float was formed by template-free spontaneous organization of small positively charged QDs.[24] Moreover, branched CdTe 3D structures have also been successfully created by varying the growth conditions of Au/Bi catalyzed nanowires (NWs)[25,26] or with the assistance of ligands.[27] Novel chiral CdTe twisted ribbons were also fabricated, with the relief of the mechanical shear stress in assembled ribbons caused by photooxidation.[28] Evidently, the above-mentioned percolated frameworks contribute great advantages for efficient photon collection and electron transport when they

[a]*State Key Laboratory on Integrated Optoelectronics, College of Electronic Science and Engineering, Jilin University, 2699 Qianjin Street, Changchun, 130012, China. E-mail: hbsun@jlu.edu.cn; haiyu_wang@jlu.edu.cn.*
[b]*College of Physics, Jilin University, 2699 Qianjin Street, Changchun, 130012, China*
[c]*School of Materials Science and Engineering, Jilin University, 5988 People's Avenue, Changchun, 130025, China*
[d]*State Key Laboratory of Supramolecular Structure and Materials, Jilin University, 2699 Qianjin Street, Changchun, 130012, China*
[e]*Department of Chemistry, Renmin University of China, Beijing, 100872, China*

† Electronic supplementary information (ESI) available: SEM (Fig. S1) and TEM images (Fig. S2 and S3) of used CdTe NBs in the present work. See DOI: 10.1039/c1nr10121h

are used for solar cells. However, the morphologies of branched-structures are generally limited by the position of the catalysts[26]/ligands;[27] or the transition process occurring on a long time scale (over 10 h),[28] *etc.* Therefore, in order to obtain percolation networks with high light harvesting efficiencies and high connectivity, an efficient and easy method for the controlled assembly of QDs into 3D nanostructures is still greatly desired for solar cell applications.

In a solar cell system, the efficiency of photovoltaic conversion strongly depends on the exciton recombination rate,[3,29–32] while in an efficient exciton generation system,[3,4,33] Auger recombination induced by exciton–exciton interactions will decrease the rate of charge separation and thus the short circuit current. It is necessary to study the exciton–exciton interaction dynamics for a deep understanding of the exciton transport and charge separation processes. However, to our knowledge, sufficient investigation into exciton–exciton interaction dynamics in the self-assembled mesocrystals is still lacking.

In this work, we demonstrate a novel QD based 3D luminescent bundle structure, namely CdTe nanobundles (NBs), constructed by thioglycolic acid (TGA)-capped CdTe QDs through a convenient and quick self-assembly route. Compared with the reports referenced above, our results present some new features: (i) a hierarchical self-assembly process is observed in the CdTe QD solution besides self-assembling into nanowires (NWs); (ii) with a rather simple hydrothermal approach, very uniform CdTe NBs can be obtained and dispersed homogeneously in solvent; (iii) the optical properties of pristine QDs are well inherited by the formed NBs. By considering the polycrystalline phase of NBs, the quantum confinement effect is contained in the formed NBs due to good separation of pristine QDs in the NBs; (iv) importantly, through transient absorption experiments, the Auger recombination in CdTe NBs is found to be extremely suppressed, due to the percolated structure of the carrier transport in NBs. Based on these features, the novel bundle-like CdTe nanostructures would exhibit great potential for solar cell applications.

2. Experimental

2.1 Preparation of 3-D CdTe nanostructures

TGA-capped CdTe QDs in aqueous solution were synthesized according to ref. 34, with a TGA : Cd^{2+} molar ratio of 1 : 1.6. The pristine QD solution was mixed with acetonitrile with a volume ratio of 1 : 5. The disturbed solution was centrifuged at 6000 rpm for 15 min. The upper clear solution was removed and the colorful precipitates were redissolved in pure water (Millipore, Mili-Q Academic) with the same concentration as pristine QDs. The elemental analysis from energy-dispersed X-ray spectrometry indicates that the ratio between Cd and S in the QDs increases from 1.2 to 2.0 after the process of acetonitrile precipitation and redissolution, indicating the partial removal of stabilizers. Then, the redissolved solution was incubated in an 80 °C water bath for 5 h. After that, the solutions were removed and then studied.

2.2 Characterization

The luminescence quantum yields (QYs) of the QDs and NBs were determined at room temperature, using Rhodamine B as the reference. UV-vis absorption and luminescence spectra were recorded using SHIMADZU UV-1700 and SHIMADZU RF-5301PC spectrophotometers, respectively. TEM images were observed with a Hitachi H-8100 microscope with an accelerating voltage of 200 kV. HR-TEM images were taken using a JEOL JEM-2100F with an accelerating voltage of 200 kV. SEM images were obtained with a SKOEL Jeol-7500F.

2.3 Time-resolved spectroscopy

Time-resolved transient absorption spectra were measured using femtosecond pump–probe experiments.[35] Samples were excited at 400 nm by the second harmonic of an amplified modelocked Ti:Sapphire laser (Millennia, Tsunami and Spitfire, Spectra-Physics). The excitation intensity of laser pulses was 2–50 μW and the repetition rate was set at 125 Hz using a synchronized optical chopper (Newport Model 75160). The intensities of the pump pulses were measured with a laser power meter (Sanwa LP1). Absorption transients were probed by delayed pulses of a femtosecond white-light continuum (420–750 nm) generated by focusing a fundamental laser pulse (800 nm) into a H_2O/D_2O cell and detected by a spectrometer (Avantes AvaSpec-2048 × 14). The group velocity dispersion of the whole experimental system was compensated by a chirp program. To avoid degradation, the sample was flowed in a cycle by a micro pump with a path length of 2 mm. All of the measurements were preformed at room temperature.

3. Results and discussion

In the self-assembly process of CdTe QDs, the curing temperature and incubation time play important roles in the formation of hierarchical structures. Generally, assembly at low temperatures would take a long time to form shape-perfect architectures, and at high temperatures would quickly cause the formation of bulk aggregates. In this work, the optimum temperature was found to be 80 °C, so the temperatures of all of the experiments were fixed at 80 °C, (Fig. S1†), at which the CdTe NBs could be formed in a short time. Fig. 1 shows the SEM images of CdTe NBs which were obtained with a 5 h incubation. Obviously, the CdTe NBs are of uniform shape and are well dispersed (Fig. 1a). The magnified image (Fig. 1b) shows that the length of the bundles is several microns along the NWs. Statistical analysis gives a length distribution of 4.5–9.5 μm, with an average length of ~6 μm (Fig. 1c) and a width distribution of 75–240 nm, with an average width of ~120 nm. Based on these statistical results, the average length-to-width ratio is established to be ~50. It is worthwhile pointing out that such a high aspect ratio is of benefit to the increased interactive area for light harvesting. The size of each NW is big enough to induce the intense scattering of incident light, which would also contribute to effective light absorption. Interestingly, it is clearly identified in the SEM image of a single CdTe NB that the NBs are constructed by the fusion of NWs on their center part (Fig. 1d).

To study the self-assembly process, a time-resolved observation was carefully performed by TEM. As shown in Fig. 2, TGA-capped CdTe QDs with an average particle size of ~3 nm were prepared according to published work (Fig. 2a).[34] After the partial removal of TGA by adding acetonitrile to the QD

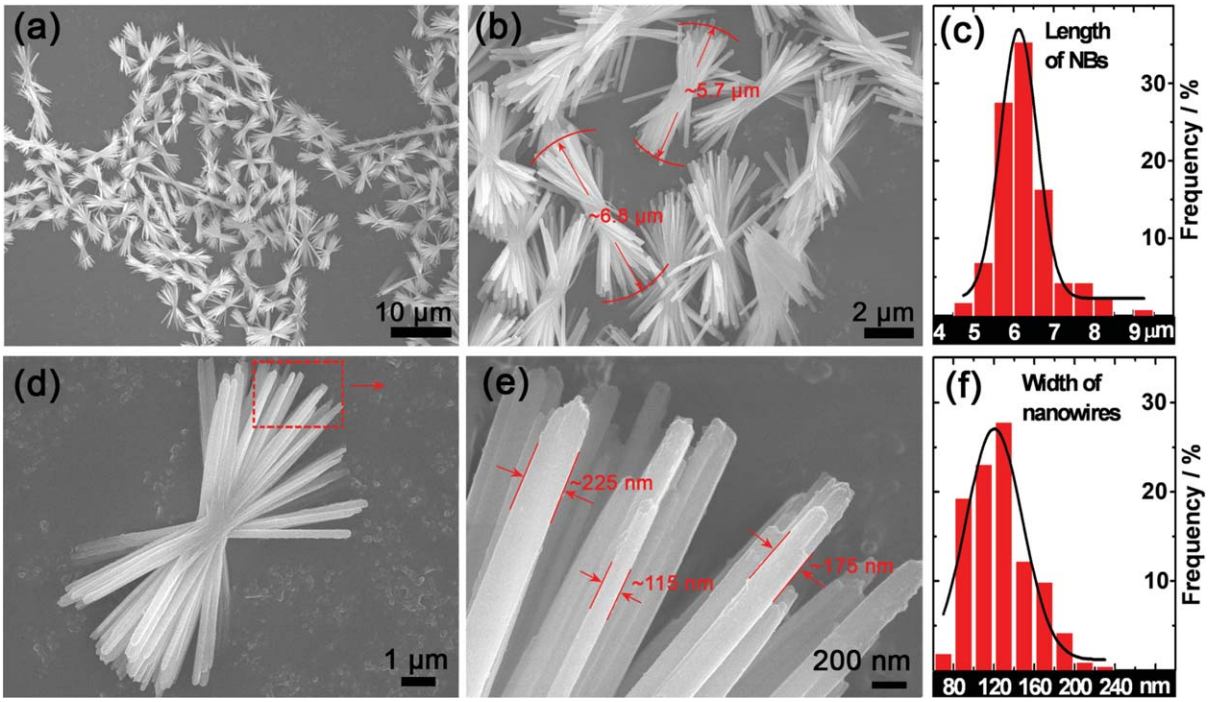

Fig. 1 a and b) SEM images of CdTe NBs; c) statistical analysis of the length of NBs; this length distribution was calculated based on two hundred NBs; d) an SEM image of one typical CdTe nanobundle; e) a magnified SEM image of one side of a NB; f) statistical analysis of the width of the nanowires; this width distribution was calculated based on five hundred nanowires.

solution, redissolved CdTe QDs could self-assemble with each other due to the strong dipole–dipole interaction.[21,36] In the early stage, the QDs aggregated together, forming a pearl-necklace structure (Fig. S2†), as previously reported by the Kotov group.[21] Then, the recrystallization process was accelerated by heating enhanced Ostwald ripening, and subsequently CdTe NWs with high aspect-ratio were formed within 25 min (Fig. 2b). With the increase in the amount of NWs in the solution, the NWs oriented

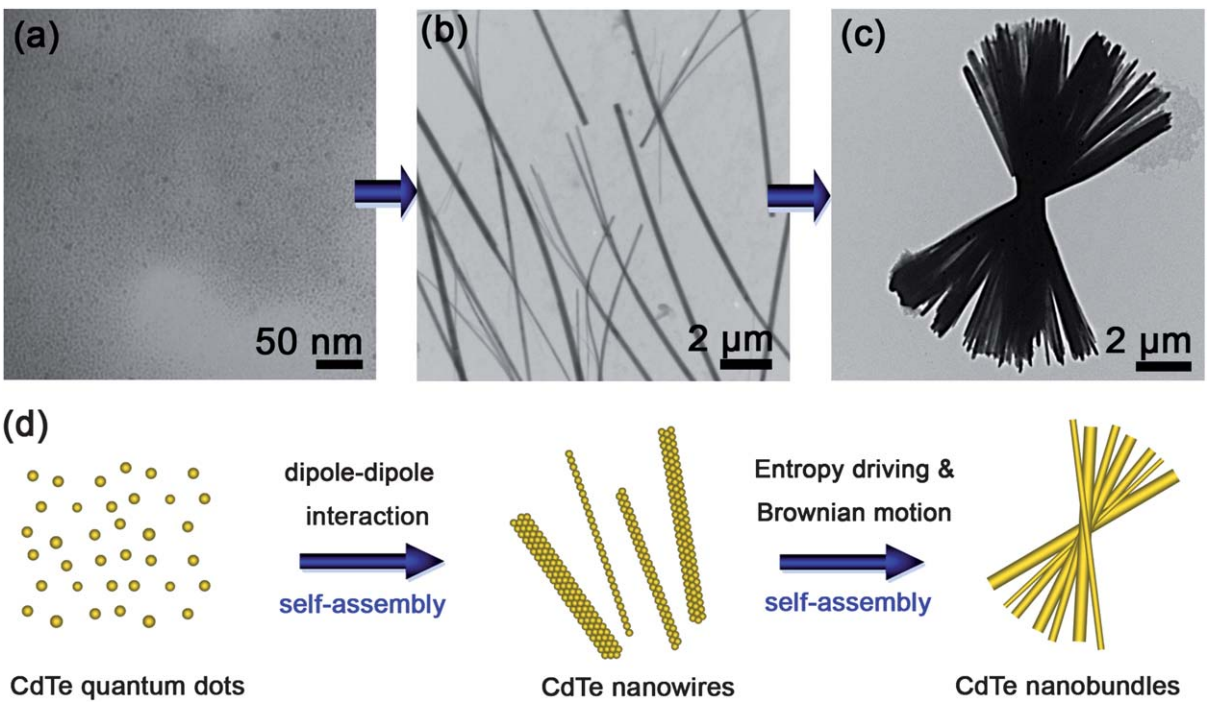

Fig. 2 a) A TEM image of as-synthesized CdTe QDs; b) a TEM image of CdTe nanowires assembled from QDs; c) a TEM image of a CdTe nanobundle assembled from nanowires; d) a scheme for the hierarchical assembly of CdTe QDs into nanobundles.

along their long-axes to form next order structures, clusters of NWs (Fig. 2b). The thermodynamic stability of these ordered structures arises from a gain in translational entropy that overrules the loss of orientational entropy associated with NW alignment.[37] With continuous incubating, the NWs became broader and thus more rigid. The harder NWs twirled around an axis along the perpendicular bisector of the fibers, due to Brownian motion. The twirling NWs underwent a competition between spinning and parallel alignment. During this process, thermally induced recrystallization would cause fusion on the connecting point of each NW, and a bundle-like CdTe nanostructure finally formed (Fig. 2c). A scheme for the hierarchical assembly of CdTe QDs into NBs is shown in Fig. 2d. The whole self-assembly process takes only a few hours. Further increasing the incubation time would result in the formation of single crystals (Fig. S3†), accompanied by a decrease in QY, in which there may be no superiority of light harvesting over one-dimensional nanostructures.

In order to further investigate the crystalline structure of the CdTe NBs, the sample was also characterized by HR-TEM (high resolution TEM). As shown in Fig. 3a, the nanobundle structures could be clearly observed from the images. A magnified image taken from the end of a bundle confirms that the bundle is constructed of separated NWs (Fig. 3b). The HR-TEM image in Fig. 3c shows that the nanowire is not a single crystal, the whole fiber is built up from nanometre sized polycrystals, indicating the formation of mesocrystals. The lattice spacing of the building units is 3.75 Å and 3.52 Å, which corresponds to the (002) and (101) planes in the hexagonal phase of CdTe, respectively. Based on the size and lattice information, it is confirmed that the pristine CdTe QDs are the basic building blocks of the nanobundle structures (red circle in Fig. 3d).

So far, it is clear that NBs are formed by a hierarchical self-assembly process, which is firstly observed in water soluble TGA-CdTe QDs. Mainly, the sequence is QDs to NWs to NBs. The same principle of self-assembly is applicable to QDs of different sizes, but the mixing ratio and incubation times are slightly different. This mesocrystal structure is important for solar cell applications, because the photogenerated excitons in NBs have a much longer diffusion length than in pristine QDs, due to the strongly reduced distance between building units. Further optical properties were studied by steady state and transient state experiments.

Fig. 4 shows UV-vis absorption and luminescence spectra of the pristine QDs and the formed CdTe NBs. A 10 nm red-shift

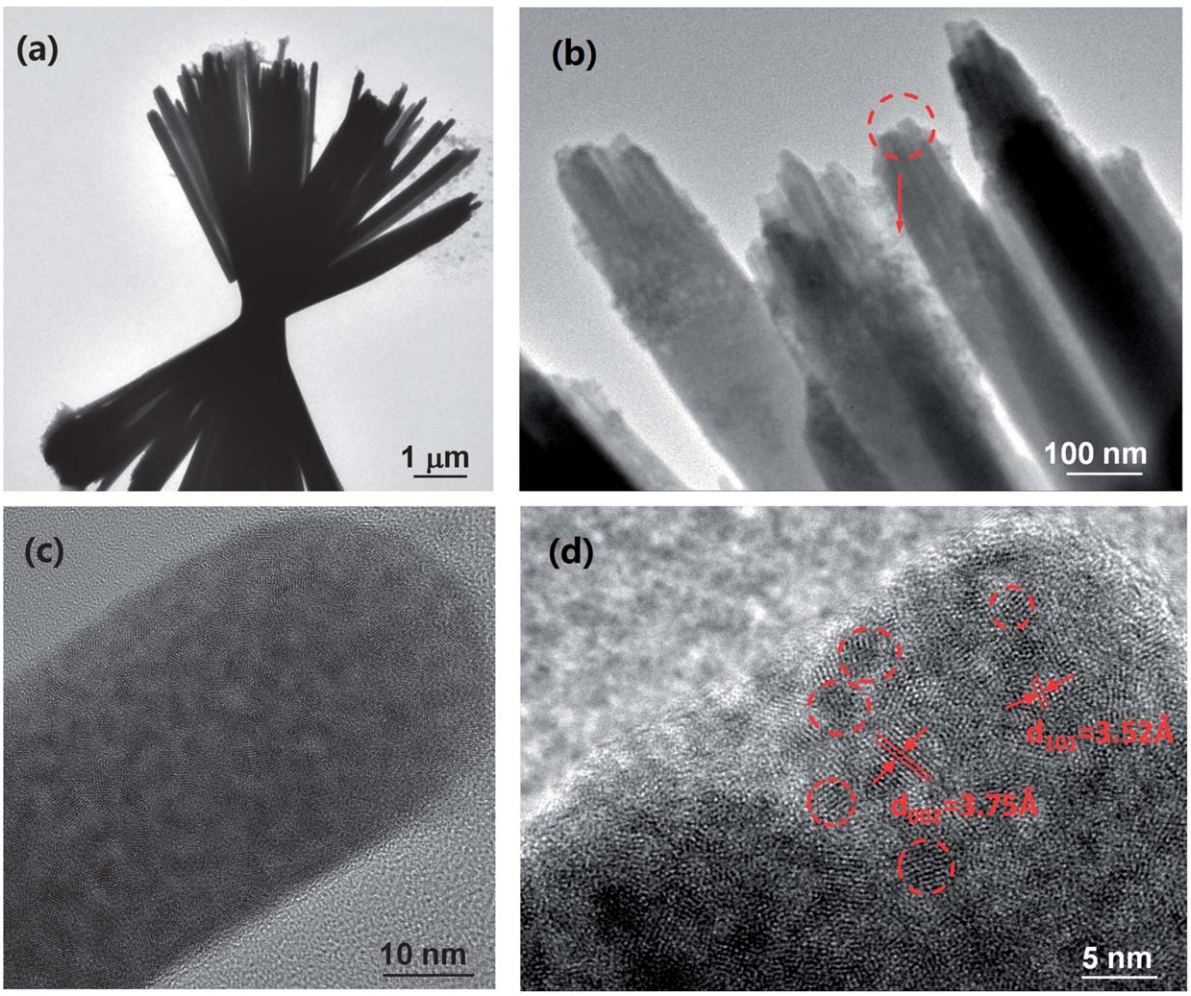

Fig. 3 TEM investigation of CdTe NBs. a) A TEM image of a CdTe NB; b) a TEM image of the NWs on the side of a CdTe NB; c and d) HR-TEM images of NWs.

was observed in both absorption and luminescence spectra of NBs compared with pristine QDs (Fig. 4a), which can be explained by the decrease of the confinement effect in NBs. The QY of the NBs was estimated to be 28%, which is much smaller than that of pristine QDs (51%). The reasons for the QY decrease in NBs are considered to be the loss of the surface-capping ligands and the formation of defects between the building blocks (QDs or NWs) of the NBs. Notably, as exhibited in Fig. 4b, the luminescence of NBs is strong enough to be observed by luminescence microscopy under halogen lamp excitation. The steady state optical properties of each QD have been well inherited after the QDs become the building units of NBs. This means that the quantum confinement properties are still in effect, although the volume of the materials increases. The inheritance of physical properties may be a speciality of QD based mesocrystals.[38] Therefore, there is scope for more investigations into the design of self-assembled mesocrystals.

To investigate the mechanism of charge transport in both QDs and NBs, transient absorption spectra were individually examined as a function of pump intensity (Fig. 5). The average number of excitons per QD, $<N(0)>$, was calculated by the equation $<N(0)> = j_p\sigma_0$, where j_p is the pump photon fluence and σ_0 is the QD absorption cross section.[4,39] In Fig. 5a, the normalized absorption changes at the first excitonic peak, $-\Delta OD/\alpha_0$ of QDs and NBs, were plotted against $<N(0)>$, where

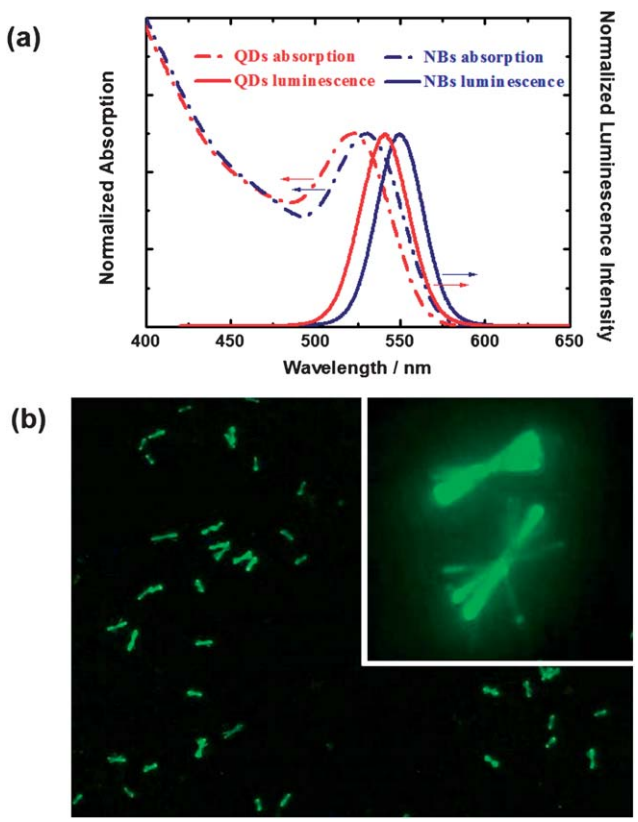

Fig. 4 a) Absorption (blue and red dash dots) and luminescence spectra (blue and red solid lines) of CdTe QDs (red lines) and NBs (blue lines). A 10 nm red-shift was observed in both the absorption and luminescence spectra of NBs compared with pristine QDs; b) a luminescence microscopic image of the CdTe NBs, inset is the magnified image of two NBs.

ΔOD and α_0 are the minimum bleaching absorbance and the ground-state absorbance at the first excitonic peak, respectively. For QDs, the absorbance change is not linear at high excitation intensities, due to the limited absorption cross section. Therefore, the excitation intensity dependence of the bleaching change in QDs is numerically analyzed by a phenomenological expression, $-\Delta OD/\alpha_0 = (k_1 \times <N(0)>)/(k_2 + <N(0)>)$, with the empirical parameters $k_1 = 0.31$ and $k_2 = 1.2$.[4] A linear relationship with a slope of 0.15 was empirically observed in NBs. This can be explained by the large volume of each NB, and thus the enhanced individual absorption cross section. The average population dynamics $<N(t)>$ are obtained from the absorbance change $\Delta OD(t)$ using the above linear and nonlinear expressions. The population dynamics of pristine QDs and assembled NBs are shown in Fig. 5b–d. At low excitation intensities, $<N(0)> = 0.17$, the population dynamics of the QDs are fitted using a biexponential decay function with a fast decay lifetime of 15 ps (12%) and a lifetime over 5 ns (Fig. 5c) longer. The fast decay may be due to the surface trapping process. As the excitation intensity increased, an additional ps to tens of ps decay component appeared, which is due to Auger recombination when $<N(0)> > 1$.

In contrast, for the assembled NBs, the population dynamics are much more insensitive to the incident intensity, which suggests that the multi-exciton interaction is not as strong as that in the individual QDs. The amplitude of the trapping component increased to 25% because of the larger surface area and the defects between the building blocks. An additional fast recombination process is analyzed as a tens of ps to hundreds of ps decay component, Fig. 5d.

A stochastic approach is used to analyze the multi-exciton interaction process.[40] For $<N(0)> < 3$, the trapping-free dynamics can be expressed as a sum of two exponentials, which correspond to the exciton recombination and biexciton Auger recombination, respectively. Thus, the population dynamics in Fig. 5b–d are fitted by a triexponential function with a fixed trapping component. The lifetime of Auger recombination is estimated to be 5 ps for 3 nm QDs and around 200 ps for NBs. The amplitude of bi-exciton recombination increases from 20% to 52% in QDs, but shows an irregular change with increasing pump intensity in NBs. Under high pump intensity ($<N(0)> > 0.17$), for both QDs and the NBs the amplitude of trapping decreases because of the band filling of the trapping state.

The life time of Auger recombination in QDs is consistent with a previous report.[32] For the assembled NBs, Auger recombination is significantly suppressed due to the reduction in the effective carrier density and the relative multi-particle interaction efficiency (Fig. 5b). In QDs, the induced excitons are confined in individual QDs, and the distance among them is much larger than the Förster resonant energy transfer (FRET) distance under current concentration ($R_{FRET} = 12.5$ nm for 3 nm sized QDs with a 4×10^{-6} M particle concentration).[41] Excitons must recombine inside each QD because of the long distance between QDs. On the contrary, induced excitons can diffuse in 3D in NBs owing to the excellent interconnectivity of the building units, QDs. The migration barrier in NBs is much lower because of the reduced distance and the same dielectric constant among building units. Thus, the generated excitons can easily delocalize to the surrounding building units, and then the local density of excitons is much lower than that in individual QDs at the same observing

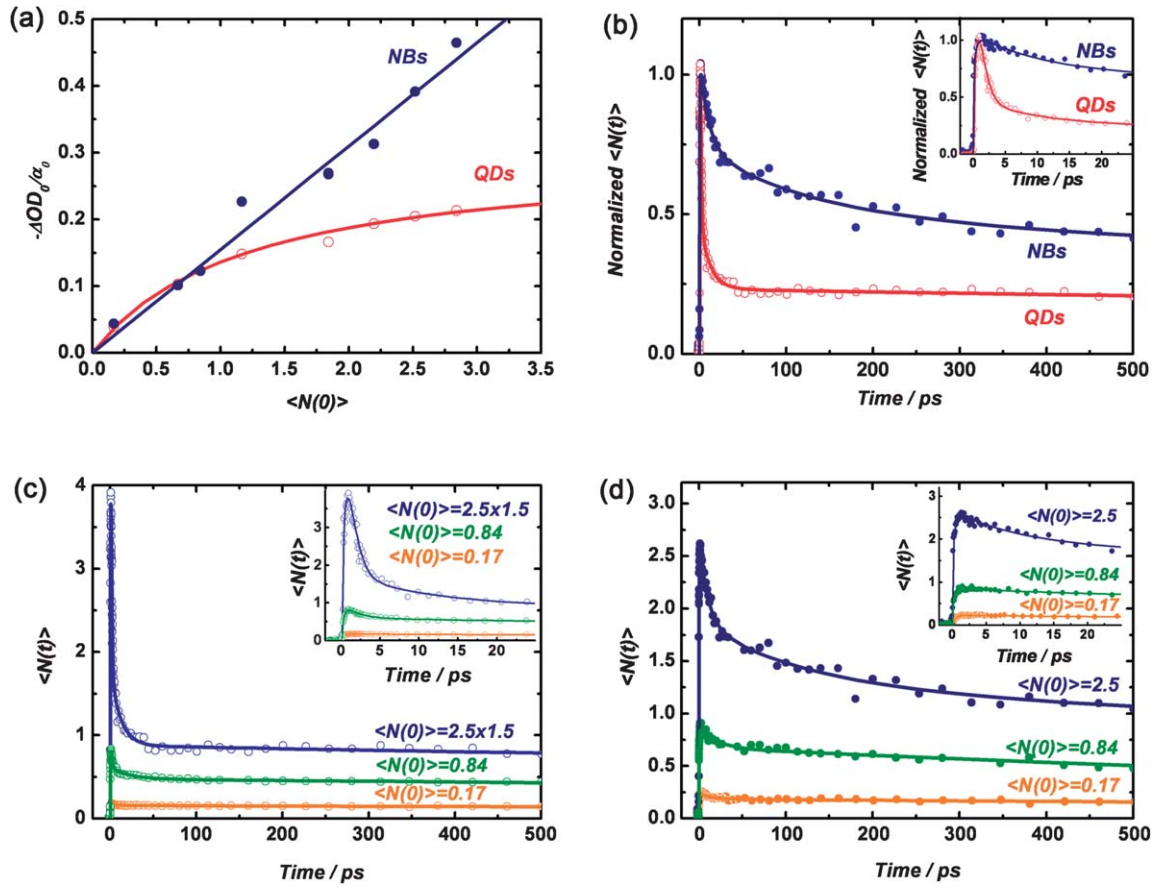

Fig. 5 a) The excitation dependence of the normalized first excitonic absorption bleaching for CdTe QDs with $D \sim 3$ nm and CdTe NBs. $<N(0)>$ is the average number of excitons per QD; b) the normalized population dynamics at the first excitonic absorption bleaching peak of CdTe QDs with $D \sim 3$ nm and CdTe NBs at pump fluences of 8.6×10^{14} ($<N(0)> = 2.5$) photon cm^{-2}. $<N(t)>$ is the average population dynamics; c) the population dynamics at the first excitonic absorption bleaching peak of CdTe QDs with $D \sim 3$ nm at pump fluences of 5.7×10^{13} ($<N(0)> = 0.17$), 2.9×10^{14} ($<N(0)> = 0.84$), 8.6×10^{14} ($<N(0)> = 2.5$) photon cm^{-2}, respectively. The dynamics at $<N(0)> = 2.5$ are multiplied as indicated in the figure for comparison; d) the population dynamics at the first excitonic absorption bleaching peak of CdTe NBs at pump fluences of 5.7×10^{13} ($<N(0)> = 0.17$), 2.9×10^{14}($<N(0)> = 0.84$), 8.6×10^{14} ($<N(0)> = 2.5$) photon cm^{-2}, respectively. Insert figures in b–d are the magnified dynamics over a short time range (0–25 ps).

time. As a result, the exciton–exciton interaction is less efficient than in individual QDs. The result of the much longer Auger recombination component, 200 ps for 50 aspect ratio, is consistent with the 100 ps Auger recombination component in a CdSe nanorod of 20 aspect ratio reported by Klimov.[42] As a summary, exciton quenching induced by Auger recombination is strongly suppressed in NBs compared with that in pristine QDs, which suggests that before exciton recombining, there is much more time remaining for charge separation in NBs than in pristine QDs.[42]

4. Conclusion

In conclusion, shape-perfect hyper-branched CdTe NBs are successfully fabricated *via* a hierarchical self-assembly process of CdTe QDs to NWs to NBs, in which the obtained nanobundle structures are constructed by CdTe QDs through nonclassical crystallization. The NBs show very high aspect ratios and are of benefit to both light harvesting and carrier separation. UV-Vis absorption and luminescence spectroscopy investigations show that the optical properties of pristine QDs are well inherited by NBs because of the polycrystalline structures. A further study by time-resolved spectroscopy suggests that the Auger recombination is dramatically suppressed in NBs compared with that in pristine QDs, which leave more time for charge separation, a key process in solar cells. Thus, hyper-branched CdTe NBs are expected to be excellent candidates for solar energy applications in the future.

Acknowledgements

This work is supported by the Natural Science Foundation, China (NSFC) under Grants No. 10904049 and the project sponsored by the Scientific Research Foundation (SRF) for the Returned Overseas Chinese Scholars (ROCS), State Education Ministry (SEM) for supports. The author also thanks Dr Lei Wang, Dr Ying Jiang and Dr Yoichi Kobayashi for helpful discussions.

References

1 C. B. Murray, D. J. Norris and M. G. Bawendi, *J. Am. Chem. Soc.*, 1993, **115**, 8706.
2 A. P. Alivisatos, *Science*, 1996, **271**, 933.
3 R. D. Schaller and V. I. Klimov, *Phys. Rev. Lett.*, 2004, **92**, 186601.

4 V. I. Klimov, A. A. Mikhailovsky, D. W. McBranch, C. A. Leatherdale and M. G. Bawendi, *Science*, 2000, **287**, 1011.
5 W. U. Huynh, J. J. Dittmer and A. P. Alivisatos, *Science*, 2002, **295**, 2425.
6 A. J. Nozik, M. C. Beard, J. M. Luther, M. Law, R. J. Ellingson and J. C. Johnson, *Chem. Rev.*, 2010, **110**, 6873.
7 P. V. Kamat and G. C. Schatz, *J. Phys. Chem. C*, 2009, **113**, 154743.
8 M. Lunz, A. L. Bradley, W.-Y. Chen, V. A. Gerard, S. J. Byrne, Y. K. Gun'ko, V. Lesnyak and N. Gaponik, *Phys. Rev. B: Condens. Matter Mater. Phys.*, 2010, **81**, 205316.
9 J. H. Bang and P. V. Kamat, *ACS Nano*, 2009, **3**, 1467.
10 M. J. Bierman and S. Jin, *Energy Environ. Sci.*, 2009, **2**, 1050.
11 I. Gur, N. A. Fromer, C.-P. Chen, A. G. Kanaras and A. P. Alivisatos, *Nano Lett.*, 2007, **7**, 409.
12 M. P. Pileni, *J. Phys. Chem. B*, 2001, **105**, 3358.
13 A. Katsuhiko, P. H. Jonathan, V. L. Michael, V. Ajayan, C. Richard and A. Somobrata, *Sci. Technol. Adv. Mater.*, 2008, **9**, 014109.
14 W. J. Kim, S. J. Kim, K.-S. Lee, M. Samoc, A. N. Cartwright and P. N. Prasad, *Nano Lett.*, 2008, **8**, 3262.
15 H. Bao, X. Cui, C. M. Li and J. Zang, *Nanotechnology*, 2007, **18**, 455701.
16 H. Bao, E. Wang and S. Dong, *Small*, 2006, **2**, 476.
17 H. Cölfen and S. Mann, *Angew. Chem., Int. Ed.*, 2003, **42**, 2350.
18 H. Cölfen and M. Antonietti, *Angew. Chem., Int. Ed.*, 2005, **44**, 5576.
19 L. Zhou and P. O'Brien, *Small*, 2008, **4**, 1566.
20 P. S. Weiss, *ACS Nano*, 2008, **2**, 1085.
21 Z. Tang, N. A. Kotov and M. Giersig, *Science*, 2002, **297**, 237.
22 H. Zhang, D. Wang and H. Möhwald, *Angew. Chem., Int. Ed.*, 2006, **118**, 762.
23 H. Niu and M. Gao, *Angew. Chem., Int. Ed.*, 2006, **45**, 6462.
24 Z. Tang, Z. Zhang, Y. Wang, S. C. Glotzer and N. A. Kotov, *Science*, 2006, **314**, 274.
25 M. Kuno, O. Ahmad, V. Protasenko, D. Bacinello and T. H. Kosel, *Chem. Mater.*, 2006, **18**, 5722.
26 J. Sun, L.-W. Wang and W. E. Buhro, *J. Am. Chem. Soc.*, 2008, **130**, 7997.
27 L. Zhang, N. Gaponik, J. Müller, U. Plate, H. Weller, G. Erker, H. Fuchs, A. L. Rogach and L. Chi, *Small*, 2005, **1**, 524.
28 S. Srivastava, A. Santos, K. Critchley, K.-S. Kim, P. Podsiadlo, K. Sun, Jaebeom Lee, C. Xu, G. D. Lilly, S. C. Glotzer and N. A. Kotov, *Science*, 2010, **327**, 1355.
29 Y. Zhang, P. Jing, Q. Zeng, Y. Sun, H. Su, Y. A. Wang, X. Kong, J. Zhao and H. Zhang, *J. Phys. Chem. C*, 2009, **113**, 1886.
30 S. Malkmus, S. Kudera, L. Manna, W. J. Parak and M. Braun, *J. Phys. Chem. B*, 2006, **110**, 17334.
31 T. W. Roberti, N. J. Cherepy and J. Z. Zhang, *J. Chem. Phys.*, 1998, **108**, 2143.
32 Y. Kobayashi, L. Pan and N. Tamai, *J. Phys. Chem. C*, 2009, **113**, 11783.
33 R. J. Ellingson, M. C. Beard, J. C. Johnson, P. Yu, O. I. Micic, A. J. Nozik, A. Shabaev and A. L. Efros, *Nano Lett.*, 2005, **5**, 865–871.
34 N. Gaponik, D. V. Talapin, A. L. Rogach, K. Hoppe, E. V. Shevchenko, A. Kornowski, A. Eychmüller and H. Weller, *J. Phys. Chem. B*, 2002, **106**, 7177.
35 Y. Jiang, H.-Y. Wang, L.-P. Xie, B.-R. Gao, L. Wang, X.-L. Zhang, Q.-D. Chen, H. Yang, H.-W. Song and H.-B. Sun, *J. Phys. Chem. C*, 2010, **114**, 2913.
36 M. Shim and P. Guyot-Sionnest, *J. Chem. Phys.*, 1999, **111**, 6955.
37 N. R. Jana, *Angew. Chem., Int. Ed.*, 2005, **43**, 1536.
38 H. Chen, V. Lesnyak, N. C. Bigall, N. Gaponik and A. Eychmuller, *Chem. Mater.*, 2010, **22**, 2309.
39 W. Yu, L. Qu, W. Guo and X. Peng, *Chem. Mater.*, 2003, **15**, 2854.
40 A. V. Barzykin and M. Tachiya, *J. Phys.: Condens. Matter*, 2007, **19**, 065105.
41 R. Osovsky, A. Shavel, N. Gaponik, L. Amirav, A. Eychmüller, H. Weller and E. Lifshitz, *J. Phys. Chem. B*, 2005, **109**, 20244.
42 H. Htoon, J. A. Hollingworth, A. V. Malko, R. Dickerson and V. I. Klimov, *Appl. Phys. Lett.*, 2003, **82**, 4776.

